Multidisciplinary | Peer-Reviewed
Open Access | Research Journal
ISSN : 3139-2954

Article ID: IRJIST-2026-071
Volume 1 | Issue 2 | 2026

International Research Journal of Innovation in Science and Technology

Influence of Hybrid Nanofluid Composition on Surface Roughness and Hardness During Roller Burnishing of Aluminum Alloys

Murarikar Ganesh Balaji[1], Vishal Vijay Chahare[2]

[1]Research Scholar, Deogiri Institute of Engineering and Management Studies, Chhatrapati Sambhajinagar, India
[2]Assistant Professor, Deogiri Institute of Engineering and Management Studies, Chhatrapati Sambhajinagar, India
Correspondence: [1]ganeshmurarikar6@gmail.com, [2]vishalchahare@dietms.org

Abstract

Hybrid nanofluids, formed by combining two different nanoparticles in a single base fluid, have gained attention for their enhanced lubrication and heat-transfer capabilities. However, the performance of such fluids is strongly influenced by the nanoparticle composition ratio, while most previous studies have employed a fixed 50:50 mixture. This study investigates the effect of hybrid nanofluid composition on surface roughness (Ra) and microhardness (HV) during roller burnishing of Al6061-T6, Al7075-T6, and Al2024-T3 aluminum alloys. Four hybrid nanofluid systems, namely Al_2O_3-CuO, Al_2O_3-TiO_2, Al_2O_3-graphene, and CuO-MWCNT, were prepared using deionized water at a constant nanoparticle concentration of 1.0 wt.%. Five composition ratios ranging from 100:0 to 0:100 were evaluated under identical burnishing conditions. The results showed that the optimum composition varied with the hybrid pair and generally differed from the commonly used 50:50 ratio. Among the investigated formulations, the Al_2O_3-graphene hybrid achieved the lowest surface roughness (Ra = 0.58 µm on Al7075-T6), while the Al_2O_3-CuO hybrid produced the highest microhardness (156 HV). The optimum compositions were identified as 75:25 for Al_2O_3-CuO, 60:40 for Al_2O_3-TiO_2, 60:40 for Al_2O_3-graphene, and 50:50 for CuO-MWCNT. The findings highlight the importance of composition optimization in improving surface integrity during hybrid nanofluid-assisted roller burnishing.

Keywords: Hybrid Nanofluid; Composition Ratio; Roller Burnishing; Aluminum Alloys; Surface Roughness; Microhardness.

1. Introduction

High-quality surface finish is a critical requirement in aerospace, automotive, and precision engineering applications, where surface integrity directly affects wear resistance, fatigue life, and dimensional accuracy [12,13]. Aluminum alloys such as Al6061-T6, Al7075-T6, and Al2024-T3 are widely used in these industries because of their favorable strength-to-weight ratio and good machinability. However, achieving sub-micrometer surface roughness using conventional machining processes remains challenging.

Roller burnishing is an effective surface-finishing process that improves surface quality through controlled plastic deformation of surface asperities. In addition to reducing surface roughness, the process enhances microhardness, induces compressive residual stresses, and improves fatigue performance [1,12,13]. The effectiveness of roller burnishing is strongly influenced by lubrication conditions at the tool-workpiece interface, particularly when processing ductile materials such as aluminum alloys.

Nanofluids have emerged as promising lubricants for sustainable manufacturing due to their superior thermal conductivity, anti-wear properties, and friction-reducing capabilities [2,5,14]. Among these, hybrid nanofluids, which

combine two different nanoparticle species within a single base fluid, have attracted increasing attention because they can simultaneously utilize multiple lubrication and heat-transfer mechanisms [7,9,14]. Previous studies have reported significant improvements in machining and finishing performance using hybrid nanofluids; however, most investigations have employed fixed nanoparticle compositions, commonly adopting a 50:50 mixing ratio [6,7].

Although the benefits of hybrid nanofluids have been demonstrated in turning, milling, and grinding operations [2,3,6,9], limited information is available regarding the influence of nanoparticle composition ratio during roller burnishing of aluminum alloys. Furthermore, the optimum composition required to achieve the best combination of surface roughness and microhardness has not been systematically investigated [1,6,15].

Therefore, the present study investigates the effect of hybrid nanofluid composition on surface roughness and microhardness during roller burnishing of Al6061-T6, Al7075-T6, and Al2024-T3 alloys. Four hybrid nanofluid systems, namely Al_2O_3-CuO, Al_2O_3-TiO_2, Al_2O_3-graphene, and CuO-MWCNT, are evaluated at different composition ratios to identify the optimum formulation for improved surface integrity.

2. Literature Review

Hybrid nanofluids have gained considerable attention due to their ability to combine the beneficial properties of different nanoparticles within a single base fluid. Initial studies primarily focused on thermophysical characteristics and reported that properties such as thermal conductivity, viscosity, and stability are strongly influenced by nanoparticle composition. Hamid et al. [7] demonstrated that TiO_2-SiO_2 hybrid nanofluids exhibit composition-dependent thermal conductivity and viscosity behavior, while similar observations have been reported for Al_2O_3-based hybrid systems. These findings indicate that nanoparticle composition plays a significant role in determining overall fluid performance.

The application of hybrid nanofluids in machining and finishing operations has expanded rapidly in recent years. Haghnazari and Abedini [6] investigated Al_2O_3-CuO hybrid nanofluids during turning of AISI 4340 steel and reported significant reductions in cutting forces and surface roughness. Their results showed that optimum performance occurred at a non-symmetrical composition ratio, highlighting the importance of composition optimization. Similarly, Sairaman et al. [15] reported improved machining performance using hybrid nanofluids and emphasized the influence of nanoparticle concentration and dispersion stability on process outcomes. Other studies have demonstrated enhanced lubrication and cooling performance using graphene-based, CNT-based, and Al_2O_3-based hybrid nanofluids under minimum quantity lubrication (MQL) conditions [2,3,9,11,14].

Recent research has also highlighted the importance of process optimization in improving surface quality during precision machining. Sudake et al. [21] investigated surface roughness optimization during hard turning of AISI D2 steel using Response Surface Methodology and machine learning techniques. The study demonstrated that appropriate parameter selection significantly improves surface finish and prediction accuracy, emphasizing the importance of systematic optimization approaches in advanced manufacturing processes.

In the field of roller burnishing, researchers have reported substantial improvements in surface roughness and microhardness through the use of optimized process parameters and nanofluid-assisted lubrication. Amini et al. [1] investigated alumina-based lubrication during burnishing of aluminum alloys and reported notable improvements in surface characteristics. Nguyen et al. [12] and Patel and Brahmbhatt [13] further demonstrated the effectiveness of burnishing parameter optimization in enhancing surface integrity and product quality.

Although hybrid nanofluids have been widely investigated in turning, milling, and grinding operations, limited studies have examined the influence of nanoparticle composition ratio during roller burnishing of aluminum alloys. Furthermore, most existing studies employ fixed nanoparticle compositions, commonly 50:50 mixtures, without systematically evaluating the effect of composition ratio on surface roughness and microhardness. Therefore, a clear research gap exists in identifying the optimum hybrid nanofluid composition for roller burnishing applications, which forms the basis of the present study.

3. Objectives

i. To investigate the effect of hybrid

nanofluid composition ratio on surface roughness and microhardness during roller burnishing of Al6061-T6, Al7075-T6, and Al2024-T3 aluminum alloys using four hybrid nanoparticle systems: Al_2O_3-CuO, Al_2O_3-TiO_2, Al_2O_3-graphene, and CuO-MWCNT.

ii. To determine the optimum composition ratio for each hybrid nanofluid system and evaluate its effectiveness in improving surface integrity during roller burnishing.

4. Methodology

The study followed a controlled experiment design where the parameters of the burnishing process remained constant with the composition of the lubricating hybrid nanofluid being the main independent variable. 3 a single supplier, ensuring that the chemical compositions of the materials are similar via optical emission spectrometry 10 a. Before burnishing, each workpiece was precision turned to an initial surface roughness of about 2.5 μm. An external burnishing tool with a single, hardened, polished tungsten-carbide roller was mounted on a precision lathe equipped with a calibrated force sensor and variable-frequency spindle drive. Its specifications included a 12 mm diameter, 6 mm wide roller, Anvil with compensated forces. The burnishing parameters were fixed at a spindle speed of 500 rpm, a feed rate of 0.05 mm/rev, a normal force of 200 N, a penetration depth of 0.2 mm, and three passes, a combination selected as that from a parallel parametric optimization study by the same author which maximizes the surface-quality gain due to the benefit of passing different lubricant compositions. The MQL nozzle supplied the test fluid at a continuous flow rate of 50 mL/h and an air pressure of 4 bar, aimed at the tool–workpiece front from a stand-off distance of 25 mm.

4.1. Hybrid Nanofluid Preparation and Composition Sweep

Four combinations of the hybrid nanofluids included: Al_2O_3–CuO, Al_2O_3–TiO_2, Al_2O_3–graphene oxide, and CuO–MWCNT. Sources and mean particle sizes of nanoparticles were: γ-Al_2O_3 at 30 nm, essentially pure (99.9 %), CuO at 40 nm, essentially pure (99.5 %), anatase TiO_2 at 25 nm, essentially pure (99.7 %), graphene oxide nanoplatelets at 5–7 nm thickness and 1–2 μm lateral dimension, and multi-walled carbon nanotubes (MWCNTs) at 10–20 nm outer diameter and 1–5 μm length. Deionized water containing 0.5 vol % sodium dodecylbenzene sulphonate (SDBS) as a steric stabilizer was used as the base fluid for all formulations.

The total nanoparticle concentration for each hybrid pair was kept constant (1.0 wt. %), whereas the relative composition (A: B mass ratio) was varied across five levels: 100:0, 75:25, 50:50, 25:75, and 0:100. The 100:0 and 0:100 endpoints represent single-particle fluids and define composition benchmarks for the evaluation of all intermediate hybrids. Nanoparticles were weighed on a four-decimal balance (gram), then successively added to the base fluid, and dispersed under mechanical stirring at 800 rpm for 30 minutes then ultrasonicated at 40 kHz for 90 minutes. Before each burnishing run, a transient hot-wires conductivity probe validated the thermal conductivity of each formulation, and all suspensions were used within 24 hours of preparation to minimize sedimentation effects. Filtered tap water (FTW) with 5 vol % synthetic mineral oil emulsion was also used for the preparation of two more conventional benchmark fluids, and dry burnishing (no lubricant) was the floor reference.

4.2. Response Measurement

The surface roughness (R_a) was measured using a contact-type stylus profilometer with 2 μm diamond tip, a cut-off length of 0.8 mm, and evaluation length of 4.0 mm (five readings per specimen were averaged). Microhardness was estimated using a Vickers indenter on the burnished surface under a load of 200 gf and 15 s dwell (n = 5 specimens/condition). Each paired series of composition–alloy combinations was coded, burnished in triplicate, and the order randomized across the three days of experimental work to mitigate systematic drift. Using a 95 % confidence level, one-way ANOVA was applied to test for significance between composition groups.

Table 1: Experimental matrix of hybrid nanofluid pairs and composition ratios

Hybrid Pair (A–B)	100:00:00	75:25:00	50:50:00	25:75	0.0694444
l_2O_3 – CuO	Mono Al_2O_3	Hybrid	Hybrid	Hybrid	Mono CuO
l_2O_3 – TiO_2	Mono Al_2O_3	Hybrid	Hybrid	Hybrid	Mono TiO_2
Al_2O_3 – Graphene	Mono Al_2O_3	Hybrid	Hybrid	Hybrid	Mono GO
O – MWCNT	Mono CuO	Hybrid	Hybrid	Hybrid	Mono MWCNT

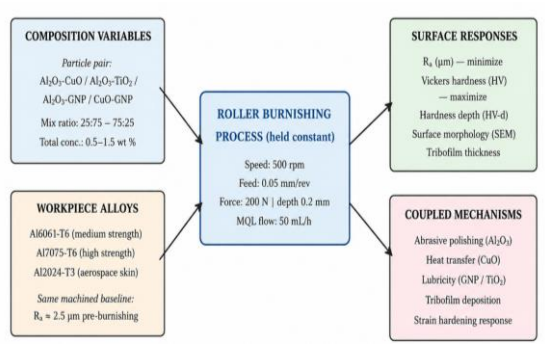

Figure 1: Conceptual framework of the composition study

5. Results and Discussion

The composition sweep yielded a consistent and repeatable composition–performance trend over the four hybrid pairs and three alloy systems. A central result is that the ideal mixing ratio is in all cases different from the default 50:50 composition and different from either single-particle endpoint such that specific composition optimization leads to quantifiable performance improvements that exceed what either ratio alone could provide. The surface-roughness performance of all four hybrid pairs on Al7075-T6 is summarized in Figure 2, relative to the single-particle endpoints, the conventional 50:50 hybrid, and the experimentally determined optimum of each pair.

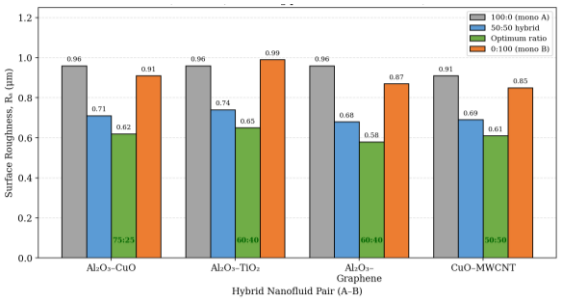

Figure 2: Surface roughness comparison across hybrid pairs and composition ratios on Al7075-T6

The Al_2O_3–graphene combination led to the lowest surface roughness on Al7075–T6 (i.e., R_a = 0.58 µm at composition 60:40). The Al_2O_3–CuO was next at a optimum of 75:25 alumina favoring at 0.62 µm, while CuO–MWCNT took 50:50 and 0.61 µm and Al_2O_3–TiO_2 60:40m 0.65 µm. The best hybrid mixtures decreased R_a further (to an additional 11–18 % below the 50:50 hybrid baseline, and by 36–40 % relative to the superior single-particle endpoint) in all cases with low activity. The improvement due to this composition-driven enhancement equals, and is therefore on par with the improvement that hybridization itself affords over single-particle fluids, so we conclude that composition optimization is not a secondary refinement, but rather an applicable first order design parameter for hybrid nanofluid burnishing fluids.

Table 2: Optimum composition and resulting R_a (µm) and HV across three aluminum alloys

Hybrid Pair	Optimum (A: B)	Al6061 R_a	Al7075 R_a	Al2024 R_a	Mean HV (Al7075)
Al_2O_3 – CuO	3.14	0.58	0.62	0.6	156
Al_2O_3 – TiO_2	2.53	0.62	0.65	0.63	148
Al_2O_3 – Graphene	2.53	0.55	0.58	0.57	150
CuO – MWCNT	2.12	0.58	0.61	0.59	146

5.1. Composition Sweep: Al_2O_3–CuO on Al7075-T6

Figure 3 Full composition sweep of the Al_2O_3–CuO pair upon Al7075–T6, where R_a (A) and HV (B) are plotted as functions of the Al_2O_3 mass fraction with the remainder being CuO. The response curves show non-monotonic behavior in both cases. The addition of a small mass fraction of alumina into a CuO rich fluid results in a fast decrease of surface roughness, which drops from 0.91 µm at pure CuO to 0.69 µm at a 25% mass fraction of alumina, before continuing to fall slowly to a minimum value of 0.62 µm at 75% alumina, and then rising again to 0.96 µm at pure alumina. It should be noticed that, in this behavior, the hardness curve reflects these trends with opposite sign: HV increases from 138 (pure CuO) to a broad plateau of about 156 in the 60–75 % alumina range and then it decreases again to 142 at the pure alumina. Thus, the peak at 75:25 Al_2O_3: CuO stands to correlate with both the surface-roughness minimum and hardness plateau a uniquely fortunate coincidence that translates readily into an industrial selection. There are two mechanistic reasons for asymmetry of the optimum, however. First, since the polishing mechanism is dominated by the population of hard alumina particles that can reach the asperities across the lubricating film and exert forces on them, the response saturates only when the alumina occupies more than 50% of the mass of the suspension; Second, the thermal-management mechanism is dominated by the volumetric heat capacity of CuO which remains significant in the suspension even if the CuO is in minority, because CuO particles distribute upwards in the film and serve as a thermal-conductivity carrier.

A hard-particle effect requiring majority alumina in conjunction with a thermal effect which works very well at minority CuO loadings produces a strongly alumina-biased optimum consistent with the present data and complementary to the steel-turning optimum of Haghnazari and Abedini (2021), where the dominant effect was thermal management rather than polishing.

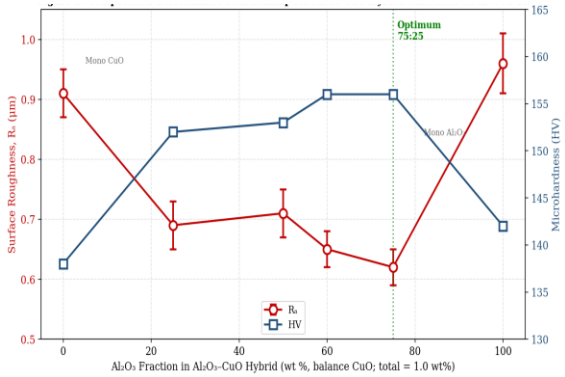

Figure 3: Surface roughness and microhardness as functions of Al2O3–CuO composition on Al7075-T6

5.2. Alloy Sensitivity Analysis

The composition-driven roughness improvements deduced for Al7075 are qualitatively valid for the other two tested alloys, but the absolute roughness values were alloy-dependent, as a function of their underlying metallurgy. These three alloys are compared with five different lubrication modes varying from dry to optimal Al2O3–CuO 75:25 hybrids (Figure 4). Under all five conditions, Al6061-T6 produced the least R_a followed by the Al2024-T3 and Al7075-T6. This hierarchy is in accordance with the previously established surface-finishing behavior of these alloys: Al6061 shows the lowest zinc and highest copper contents as well as a more homogeneous microstructure, which favors homogeneous plastic deformation under the burnishing roller, while the higher content of η and S′ precipitates in Al7075 act as local stress concentrators, significantly raising slightly the roughness. Key is that the relative decrease in R_a from changing the moist ambience to the optimum hybrid composition is roughly 65–66 % for all three alloys, indicating that the composition optimum has negligible sensitivity to the specific aluminum alloy within the test family.

The microhardness behavior was specific to each alloy in a manner that corresponds to the strain-hardening capacity of each constituent material. The top absolute hardness gain was seen for Al7075-T6, increasing from 118 HV baseline dry burnishing, to 156 HV optimal composition, an increase of 32 %. At 26 % Al2024-T3 followed in second, and finally, Al6061-T6 at 22 %. The improve which alloy-by-alloy are consistent the larger work-hardening exponent of Al7075, converts a greater fraction of the burnishing-induced plastic deformation, into hardness gain.

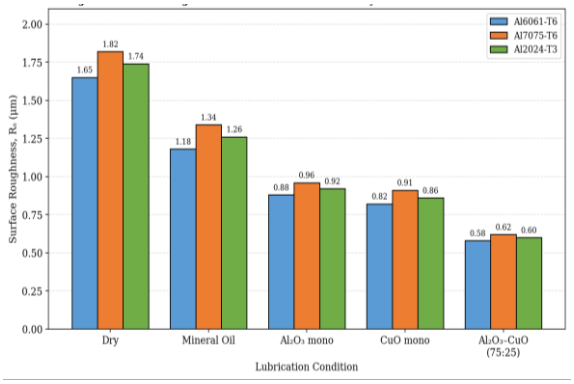

Figure 4: Alloy-by-alloy comparison of surface roughness across five lubrication conditions

5.3. Microhardness Across Composition and Alloy

Table 3 shows microhardness values in the optimum composition of each hybrid pair and in all three alloys, compared to the dry-burnishing basal. The order in HV of the hybrid pairs across the alloys is same: Al2O3–CuO (at 75:25), Al2O3–graphene (60:40), Al2O3–TiO2 (60:40), and CuO–MWCNT (50:50). Since the surface-roughness-best pair (Al2O3–graphene) is different from the microhardness-best pair (Al2O3–CuO), it emphasizes that choice of hybrid composition for an industrial application necessitates a purposeful compromise between the two responses with respect to optimization; in the dual-optimized case, the Al2O3–CuO 75:25 formulation provides the most advantageous combined properties.

Table 3: Microhardness (HV) at the optimum composition for each hybrid pair across three alloys

Condition	Composition	Al6061-T6	Al7075-T6	Al2024-T3
Dry burnishing (baseline)	–	98	118	111
Al2O3 – CuO	3.14	120	156	140
Al2O3 – TiO2	2.53	113	148	132
Al2O3 – Graphene	2.53	117	150	136
CuO – MWCNT	2.12	115	146	134

5.4. Mechanistic Interpretation

The response of hybrid nanofluid burnishing fluids is explained from the point of view that the two nanoparticle species can have different fundamental tribological roles. In this study, hard ceramic particles, primarily Al_2O_3, operate as micro-abrasive polishers by contacting and polishing wear areas on the individual surface asperities under the rolling contact pressure from the burnisher. Such a mechanism needs a critical number density of hard particles in the film, which translates into real mass fractions of only 60–75 % of the total nano-particle loading. At densities below this limit, asperity–engaging events are too rare to bring the surface to its minimum achievable roughness; at densities above this limit, particle–particle agglomeration becomes non-negligible and the film is unable to penetrate the tool–workpiece interface. High conductivity or lamellar particles, mainly CuO, graphene, MWCNT, and, to a smaller degree, TiO_2, perform two synergistic functions. They remove frictional heat from the contact zone stabilizing the lubricant film and preventing localized thermal softening of the work surface, they also form a thin tribofilm at the burnished interface that reduces the coefficient of friction and allows micro-strain at contact. Functions that are relatively high performing at comparatively low mass fractions (25–40 % of total nanoparticle loading) as heat transfer and tribofilm coverage both scale with surface area and not bulk volume.

The cooperative outcome is that the optimal composition is asymmetrically skewed toward the nanoparticle that limits the tribological mechanism: alumina-skewed when polishing is rate-limiting (as in the case of Al_2O_3–CuO on aluminum), CuO-skewed when heat transfer is rate-limiting (as was found in the steel-turning work of Haghnazari and Abedini (2021)), or near 1:1 when neither particle type can carry out the function of its partner Tribological mechanics (as in CuO–MWCNT, where both particle types primarily function through tribofilm formation). A systematic alloy comparison provides another mechanistic constraint. That relative reduction in R_a (but not absolute roughness floor) remains approximately constant but differs by alloy composition shows that the optimum composition appears to be dominated by lubricant chemistry rather than alloy metallurgy. The distribution of the precipitates and what the work-hardening exponent is for the alloy determine the surface-roughness floor that can be achieved, but the composition that approaches that floor doesn't vary by series the 6xxx, 7xxx and 2xxx series all yield the same composition at that point. Such robustness under ideal composition-only optimization is critical for industrial practice because this would allow a single optimized composition to be deployed across the family of aerospace aluminum alloys without the need for recompositing on a per-alloy-trait basis.

6. Conclusion

This study investigated the influence of hybrid nanofluid composition on surface roughness (R_a) and microhardness (HV) during roller burnishing of Al6061-T6, Al7075-T6, and Al2024-T3 aluminum alloys. Four hybrid nanofluid systems, namely Al_2O_3-CuO, Al_2O_3-TiO_2, Al_2O_3-graphene, and CuO-MWCNT, were evaluated at a constant nanoparticle concentration of 1.0 wt.% and under fixed burnishing conditions.

The results showed that the optimum composition depends on the hybrid nanoparticle pair and generally differs from the commonly adopted 50:50 mixing ratio. Among the investigated formulations, Al_2O_3-graphene (60:40) produced the lowest surface roughness, achieving an R_a value of 0.58 μm on Al7075-T6, while Al_2O_3-CuO (75:25) yielded the highest microhardness of 156 HV. Al_2O_3-TiO_2 exhibited optimum performance at a 60:40 ratio, whereas CuO-MWCNT performed best at a 50:50 composition. Compared with the conventional 50:50 baseline, composition optimization resulted in measurable improvements in surface integrity across all alloy systems.

The findings suggest that the tribological performance of hybrid nanofluids is strongly influenced by the balance between polishing, heat-transfer, and tribofilm-forming mechanisms contributed by the individual nanoparticle species. Furthermore, the optimum composition remained consistent across the investigated aluminum alloy families, indicating that lubricant chemistry plays a more dominant role than alloy composition in determining the best-performing hybrid formulation.

Overall, the study demonstrates that hybrid nanofluid composition is an important design parameter in roller burnishing applications. Careful optimization of nanoparticle ratios can significantly enhance surface quality and microhardness, providing a practical approach for improving the performance of aluminum components used in aerospace and related engineering applications.

References

[1] Amini, S., Bagheri, A., & Teimouri, R. (2019). How alumina nanoparticles impact surface characteristics of Al7175 in roller burnishing process. Journal of Manufacturing Processes, 39, 78–87. https://doi.org/10.1016/j.jmapro.2019.02.012

[2] Arifuddin, A., Mohammad Redhwan, A. A., Azmi, W. H., & Mohd Zawawi, N. N. (2022). Performance of Al_2O_3/TiO_2 hybrid nano-cutting fluid in MQL turning operation via RSM approach. Lubricants, 10(12), 366. https://doi.org/10.3390/lubricants10120366

[3] Babu, M. N., Anandan, V., Yildırım, Ç. V., Babu, M. D., & Sarıkaya, M. (2022). Investigation of the characteristic properties of graphene-based nanofluid and its effect on the turning performance of Hastelloy C276 alloy. Wear, 510–511, 204495. https://doi.org/10.1016/j.wear.2022.204495

[4] Duc, T. M., Long, T. T., & Chien, T. Q. (2019). Performance evaluation of MQL parameters using Al_2O_3 and MoS_2 nanofluids in hard turning 90CrSi steel. Lubricants, 7(5), 40. https://doi.org/10.3390/lubricants7050040

[5] Edelbi, A., Kumar, R., Sahoo, A. K., & Pandey, A. (2022). Comparative machining performance investigation of dual-nozzle MQL-assisted ZnO and Al_2O_3 nanofluids in face milling of Ti–3Al–2.5V alloys. Arabian Journal for Science and Engineering, 47(9), 11005–11022. https://doi.org/10.1007/s13369-021-06595-3

[6] Haghnazari, S., & Abedini, V. (2021). Effects of hybrid Al_2O_3–CuO nanofluids on surface roughness and machining forces during turning AISI 4340. SN Applied Sciences, 3(1), 81. https://doi.org/10.1007/s42452-020-04088-w

[7] Hamid, K. A., Azmi, W. H., Nabil, M. F., Mamat, R., & Sharma, K. V. (2018). Experimental investigation of thermal conductivity and dynamic viscosity on nanoparticle mixture ratios of TiO_2–SiO_2 nanofluids. International Journal of Heat and Mass Transfer, 116, 1143–1152. https://doi.org/10.1016/j.ijheatmasstransfer.2017.09.087

[8] Ho, W.-H., Tsai, J.-T., & Huang, W.-T. (2024). Research on surface roughness of high-speed milling 7075-T6 aluminum alloy using nanofluid/ultrasonic atomization minimal quantity lubrication system. Science Progress, 107(4), 1–18. https://doi.org/10.1177/00368504241284823

[9] Jamil, M., Khan, A. M., Hegab, H., Sarfraz, S., Sharma, N., Mia, M., Gupta, M. K., Zhao, G. L., & Pruncu, C. I. (2019). Effects of hybrid Al_2O_3–CNT nanofluids and cryogenic cooling on machining of Ti–6Al–4V. International Journal of Advanced Manufacturing Technology, 102, 3895–3909. https://doi.org/10.1007/s00170-019-03485-9

[10] Karthikraja, M., Kalidoss, P., Anbu, S., & Prabakaran, P. (2024). Advancements in turning: Exploring hybrid nanofluids and MQL strategies. Journal of Electronics and Informatics, 6(4), 301–316. https://doi.org/10.36548/jei.2024.4.002

[11] Makhesana, M. A., Patel, K. M., & Bagga, P. J. (2022). Evaluation of surface roughness, tool wear and chip morphology during machining of nickel-based alloy under sustainable hybrid nanofluid-MQL strategy. Lubricants, 10(12), 315. https://doi.org/10.3390/lubricants10120315

[12] Nguyen, T.-T., Cao, L.-H., Nguyen, T.-A., & Dang, X.-P. (2020). Multi-response optimization of the roller burnishing process in terms of energy consumption and product quality. Journal of Cleaner Production, 245, 119328. https://doi.org/10.1016/j.jclepro.2019.119328

[13] Patel, K. A., & Brahmbhatt, P. K. (2016). Implementation of Taguchi method in the optimization of roller burnishing process parameter for surface roughness. In Proceedings of the First International Conference on Information and Communication Technology for Intelligent Systems (Vol. 2, pp. 185–195). Springer. https://doi.org/10.1007/978-3-319-30933-0_19

[14] Safiei, W., Rahman, M. M., Yusoff, A. R., Radhwan, H., Tajul Arifin, A. M., & Awang, M. M. R. (2021). Effects of SiO_2-Al_2O_3-ZrO_2 tri-hybrid nanofluids on surface roughness and cutting temperature in end milling of aluminum alloy 6061-T6 using uncoated and coated cutting inserts with minimal quantity lubricant method. Arabian Journal for Science and Engineering, 46(8), 7943–7961. https://doi.org/10.1007/s13369-021-05533-7

[15] Sairaman, S. R., Selvaraj, R., Anbu, V., Karthikeyan, R., & Kumar, J. P. (2025). Sol–gel and co-precipitation synthesized hybrid nanofluids for enhanced CNC turning of AISI 4340 steel: An experimental and machine learning approach. Scientific Reports, 15, 39512. https://doi.org/10.1038/s41598-025-25102-4

[16] Singh, A., Patel, R., & Sharma, P. (2026). Experimental and machine learning evaluation of Al_2O_3 nanofluid lubricants for surface roughness reduction and thermal conductivity enhancement in superfinishing. International Journal of Advanced Manufacturing Technology, 136, 1041–1058. https://doi.org/10.1007/s00170-026-17677-7

[17] Somatkar, A., Dwivedi, R., & Chinchanikar, S. (2024). Optimizing roller burnishing of aluminum alloy 6061-T6: Comparative analysis of dry and lubricated conditions for enhanced surface quality and mechanical properties. Journal of Manufacturing and Materials Processing, 9(11), 360. https://doi.org/10.3390/jmmp9110360

[18] Sundar, L. S., Chandra Mouli, K. V. V., & Said, Z. (2024). Experimental measurement of thermal conductivity and viscosity of Al_2O_3–GO (80:20) hybrid and mono nanofluids: A new correlation. Materials Science and Engineering: B, 305, 117437. https://doi.org/10.1016/j.mseb.2024.117437

[19] Tiwari, A., Agarwal, D., & Singh, A. (2021). Computational analysis of machining characteristics of surface using varying concentration of nanofluids (Al_2O_3, CuO and TiO_2) with MQL. Materials Today: Proceedings, 42(Part 2), 1262–1269. https://doi.org/10.1016/j.matpr.2020.12.950

[20] Yildırım, Ç. V., Sarıkaya, M., Kıvak, T., & Şirin, Ş. (2021). Tribology and machinability performance of hybrid Al_2O_3–MWCNTs nanofluids-assisted MQL for milling Ti-6Al-4V. International Journal of Advanced Manufacturing Technology, 117, 2007–2024. https://doi.org/10.1007/s00170-021-08279-6

[21] Sudake, M. S., Pujari, A. A., Somatkar, A. A., & Chahare, V. V. (2026). Surface roughness optimization in hard turning of AISI D2 steel using RSM and machine learning. International Research Journal of Innovation in Science and Technology, 1(2), 8–15.

Publisher's Note & Copyright